Journal of Dental Research
2018, Vol. 97(1) 84–90

DOI: 10.1177/0022034517728504
journals.sagepub.com/home/jdr

# The Presence of MMP-20 Reinforces Biomimetic Enamel Regrowth

**S. Prajapati[1*], Q. Ruan[1*], K. Mukherjee[1], S. Nutt[2], and J. Moradian-Oldak[1]**

**Abstract**

Biomimetic synthesis of artificial enamel is a promising strategy for the prevention and restoration of defective enamel. We have recently reported that a hydrogel system composed of chitosan-amelogenin (CS-AMEL) and calcium phosphate is effective in forming an enamel-like layer that has a seamless interface with natural tooth surfaces. Here, to improve the mechanical system function and to facilitate the biomimetic enamel regrowth, matrix metalloproteinase–20 (MMP-20) was introduced into the CS-AMEL hydrogel. Inspired by our recent finding that MMP-20 prevents protein occlusion inside enamel crystals, we hypothesized that addition of MMP-20 to CS-AMEL hydrogel could reinforce the newly grown layer. Recombinant human MMP-20 was added to the CS-AMEL hydrogel to cleave full-length amelogenin during the growth of enamel-like crystals on an etched enamel surface. The MMP-20 proteolysis of amelogenin was studied, and the morphology, composition, and mechanical properties of the newly grown layer were characterized. We found that amelogenin was gradually degraded by MMP-20 in the presence of chitosan. The newly grown crystals in the sample treated with MMP-20–CS-AMEL hydrogel showed more uniform orientation and greater crystallinity than the samples treated with CS-AMEL hydrogel without MMP-20. Stepwise processing of amelogenin by MMP-20 in the CS-AMEL hydrogel prevented undesirable protein occlusion within the newly formed crystals. As a result, both the modulus and hardness of the repaired enamel were significantly increased (1.8- and 2.4-fold, respectively) by the MMP-20–CS-AMEL hydrogel. Although future work is needed to further incorporate other enamel matrix proteins into the system, this study brings us one step closer to biomimetic enamel regrowth.

**Keywords:** amelogenin, biomaterial(s), hydroxyapatite, matrix metalloproteinases (MMPs), remineralization, tooth

## Introduction

The mineral content of enamel consists of tightly packed arrays of elongated carbonated-hydroxyapatite (HAP) crystals that organize into an intricate interwoven structure (Nanci 2013). The elongated growth of thin ribbons of apatite crystals is mediated by enamel matrix proteins such as amelogenin, ameloblastin, and enamelin, which are secreted by ameloblasts during the secretory stage of amelogenesis (Moradian-Oldak 2012). These proteins are degraded and removed by enamel proteinases to allow completion of mineralization. Specifically, full-length amelogenin and other proteins are cleaved by matrix metalloproteinase–20 (MMP-20) soon after their secretion and eventually removed by serine proteinase kallikrein–4 during the maturation stage (Bartlett and Simmer 1999).

Biomimetic repair of tooth enamel has been identified as a promising strategy for prevention and restoration of defective enamel (Mann 1997; Palmer et al. 2008; Moradian-Oldak 2009). Compared with the current restorative materials in dentistry, biomimetic repair is expected to exhibit a better integration with tooth structures when organized enamel apatite crystals with robust attachment to the enamel surface can be grown. One route to achieve oriented enamel-like materials consists of in situ remineralization of enamel in the presence of amelogenin and other enamel matrix proteins (Ruan and Moradian-Oldak, 2015). The major protein in the developing enamel matrix, amelogenin exhibits a capacity to guide the formation of ordered bundles of HAP crystals in vitro (Beniash et al. 2005; Yang et al. 2010). Accordingly, we have developed chitosan-based hydrogel systems containing full-length amelogenin or leucine-rich amelogenin peptide for biomimetic regrowth of enamel (Ruan et al. 2013; Ruan and Moradian-Oldak 2014; Mukherjee et al. 2016). In these systems, amelogenin/peptide assemblies stabilized Ca-P clusters in the hydrogel and mediated the formation of co-aligned crystals anchored to the natural enamel substrate. A dense interface between the newly grown layer and natural enamel was formed, and the new layer exhibited increased hardness and elastic modulus compared with etched enamel. These studies demonstrated

[1]Center for Craniofacial Molecular Biology, Herman Ostrow School of Dentistry, University of Southern California, Los Angeles, CA, USA
[2]Mork Family Department of Chemical Engineering and Materials Science, University of Southern California, Los Angeles, CA, USA
*Authors contributing equally to this article.

**Corresponding Author:**
J. Moradian-Oldak, Center for Craniofacial Molecular Biology, Herman Ostrow School of Dentistry, University of Southern California, 2250 Alcazar St., Los Angeles, CA 90033, USA.
Email: joldak@usc.edu

the potential of using a protein-containing chitosan hydrogel for biomimetic reconstruction of enamel.

Considering the critical roles that proteinases play in normal enamel formation, here we introduced MMP-20 into an chitosan-amelogenin (CS-AMEL) hydrogel to further mimic the functions of enamel matrix proteinases in vitro. A recent study claimed that the MMP-20–induced proteolysis of full-length amelogenin in part regulated the transformation of amorphous calcium phosphate (ACP) into ordered arrays of enamel crystals in vitro (Kwak et al. 2016). We recently reported that MMP-20 plays a critical role in preventing protein occlusion inside enamel crystals (Prajapati et al. 2016). By investigating *Mmp20*-null mice, we showed that the absence of MMP-20 in these animals resulted in the formation of HAP crystals with defects at the nano level due to the occlusion of full-length amelogenin within them. Our recent findings, together with knowledge of the other important MMP-20 activities in dental enamel formation, have led us to hypothesize that MMP-20 proteolysis of amelogenin in a chitosan hydrogel could enhance biomimetic enamel repair by mediating crystal formation and preventing protein occlusion within the apatite crystals. To test this hypothesis, we investigated whether adding MMP-20 to CS-AMEL hydrogel has an effect on apatite crystal growth on an acid-etched enamel surface. The microstructure, orientation, composition, and mechanical performance of the newly grown layer were characterized by scanning electron microscopy (SEM), X-ray diffraction (XRD), Fourier transform infrared spectroscopy (ATR-FTIR), and nanoindentation tests. We demonstrate that adding MMP-20 to CS-AMEL hydrogel improved the mechanical properties of the newly grown layer by regulating crystal growth and preventing protein occlusion.

## Materials and Methods

### *Recombinant Amelogenin rP172 Expression and Purification*

Recombinant full-length porcine amelogenin rP172 was expressed in *Escherichia coli* and purified as described previously (Sun et al. 2006, 2008). The rP172 protein has 172 amino acids and is an analogue of the full-length native porcine P173 but lacks the N-terminal methionine as well as a phosphate group on Ser16.

### *Preparation of MMP-20–Chitosan-Amelogenin Hydrogel*

CS-AMEL hydrogel was prepared by mixing chitosan (medium molecular weight, 75% to 85% deacetylated; Sigma-Aldrich) solution (960 µL, 2% m/v), $Na_2HPO_4$ (15 µL, 0.1M), $CaCl_2$ (25 µL, 0.1M), and amelogenin rP172 (200 µg) as described previously (Ruan et al. 2014). The pH value was adjusted to 6.5 with 1M NaOH. To make MMP-20–CS-AMEL, the recombinant human enamel proteinase MMP-20 (rhMMP20, Enzo Life Sciences) was added to the CS-AMEL hydrogel (protein/MMP-20 [wt:wt] = 1,000:1) along with $ZnCl_2$ solution (20 µM) to activate the enzyme.

### *Analysis of Degradation Products of rP172 by rhMMP20*

Proteolysis of amelogenin by MMP-20 in the presence of chitosan was analyzed using high-performance liquid chromatography (HPLC) and sodium dodecyl sulfate polyacrylamide gel electrophoresis. The MMP-20–CS-AMEL hydrogel was incubated at 37 °C for 3, 6, 14, and 24 h to check for degradation of amelogenin. A C4 analytical column (Vydac) was used for detection of proteolytic products. The sample was diluted with 0.2% trifluoroacetic acid (TFA) to make it safe to perform HPLC. The peptides were eluted with buffer A (0.1% TFA) and buffer B (buffer A + 60% acetonitrile) with a gradient of B over 75 min. Liquid Chromatograph workstation version 6.41 was used for the detection of the peaks, and elution was monitored at 215 to 220 nm.

### *Tooth Slice Preparation*

Extracted human third molars (following the standard protocols at the Herman Ostrow School of Dentistry and approved by the Institutional Review Board at the University of Southern California) without any restorations were selected for the experiments. They were cut into sagittal sections (2 mm) using a water-cooled low-speed diamond saw (MTI Corporation, SYJ 150-A). The tooth slices were prepared in the following steps: 1) polishing of both sides of the tooth surfaces using a fine-grit paper followed by sonication in a water bath for 2 min, 2) immersion of the entire polished tooth slices in 30% phosphoric acid for 30 s followed by 2 to 3 washes with deionized water, and 3) 2-$mm^2$ windows were defined on the cut enamel surfaces of the tooth slices using nail varnish followed by drying for at least 4 h.

### *Biomimetic Regrowth of Demineralized Enamel*

Thirty microliters of MMP-20–CS-AMEL hydrogel were carefully applied to exposed enamel windows of the prepared tooth slices and then kept in a desiccator for 15 min. The tooth slices were then immersed in 30 mL artificial saliva solution (0.2 mM $MgCl_2$, 1 mM $CaCl_2.H_2O$, 20 mM HEPES buffer, 4 mM $KH_2PO_4$, 16 mM KCl, 4.5 mM $NH_4Cl$, pH 7.0) with a fluoride ($F^-$) concentration of 1 ppm at 37 °C for 5 d. To mimic the ionic condition in the oral environment, the artificial saliva solution was used to continually provide the $Ca^{2+}$ and $PO_4^{3-}$ ions needed during the enamel regrowth. After the allotted time, the tooth slices were removed from the solution, sonicated in a water bath for 10 min, and air dried. Chitosan-only and CS-AMEL hydrogel without MMP-20 were used as controls following the same above procedure and under the same conditions.

### *Characterization of the Newly Grown Layer on Enamel*

*Scanning Electron Microscopy.* The dried tooth slices were sputter coated with gold for 30 s, and imaging was performed in a field emission SEM (JEOL JSM-7001F) operating at an

accelerating voltage of 10 keV. The diameters of crystals in the digital SEM images were measured using Photoshop (Adobe) ($n > 50$) and expressed as mean ± standard deviation. To get a more accurate comparison, the measured positions were carefully kept the same for all measurements, at ~100 nm below the tips of the needle-like crystals.

*XRD.* The newly grown crystals were analyzed using XRD (Rigaku diffractometer, Rigaku Corporation) by scanning the tooth slices directly. The XRD with Cu $K_\lambda$ radiation ($\lambda$ = 1.542 Å) was operated at 70 kV and 50 mA with a sampling step of 0.04 and 2θ ranging from 10 to 60°. The intensities of (002), (211), and (300) peaks were measured after removing the pattern background and strip Kα2 in JADE software (Materials Data Inc., version 6.5). The degree of crystallinity was calculated using diffraction peaks (211) and (300) of HAP with the equation given as Landi et al. (2000):

$$X_c = \frac{I_{300} - V_{211/300}}{I_{300}} \times 100\%$$

where $X_c$ is the fraction of crystalline phase, $I_{300}$ is the intensity of the (300) diffraction peak, and $V_{211/300}$ is the intensity of the trough between the (211) and (300) diffraction peaks of HAP.

*ATR-FTIR.* FTIR spectra were acquired from a Nicolet 4700 Spectrometer with a Gladi-ATR diamond crystal accessory. The sample with newly grown crystals was pressed on the diamond crystal and scanned at 0.2 $cm^{-1}$ resolution, from 4,000 $cm^{-1}$ to 500 $cm^{-1}$, 36 times for each sample.

*Nanoindentation.* Hardness and elastic modulus were calculated using a nano-indenter (Agilent-MTS XP) with a Berkovich tip at a depth of 2,000 nm. Twenty-five test points in 2 different areas of enamel in each sample ($n = 4$) were measured.

*Statistical Analysis.* Enamel remineralization experiments were repeated 3 times, and mechanical tests were conducted in duplicate. The data were analyzed using Excel 2010. Single-factor analysis of variance was used to calculate the significance of the difference between the hardness and modulus of elasticity values between the samples grown in chitosan, chitosan-amelogenin, and MMP-20–CS-AMEL hydrogel. A value of $P < 0.001$ was considered statistically significant.

## Results

### *Proteolysis of Amelogenin rP172 by MMP-20 in the Chitosan Hydrogel*

Consistent with the observations in our previous studies (Sun et al. 2008; Yang et al. 2011), rP172 was gradually degraded in the CS-AMEL hydrogel by MMP-20 with increasing incubation time (Fig. 1). The HPLC results revealed that the intensity of the elution peak for full-length amelogenin decreased after 3 h of incubation. At the end of 14 h, the peak of full-length amelogenin was detectable along with another peak representing a major proteolytic product, P148 (Moradian-Oldak et al. 2001; Sun et al. 2008). After 24 h, a full-length amelogenin band along with the P148 and a band at 13 kDa persisted.

### *Biomimetic Regrowth of Etched Enamel with MMP-20–CS-AMEL Hydrogel*

When exposed to an acidic environment, the organized HAP crystals in enamel are susceptible to a demineralization process, which breaks the enamel crystals into discontinuous and fragmented pieces (Fig. 2A, B). After remineralization in artificial saliva for 5 d, needle-like crystals were formed on the etched enamel surfaces of tooth slices (Fig. 2C to H). The diameters of the newly formed crystals were 52.5 ± 6.5 nm, 45.7 ± 7.6 nm, and 42.6 ± 5.6 nm for the samples treated with chitosan only, CS-AMEL, and MMP-20–CS-AMEL hydrogels, respectively. In the samples treated with chitosan hydrogel (Fig. 2C, D), the apatite crystals appeared more heterogeneous, with varying lengths and orientations. In comparison, homogenous and uniformly oriented crystals were formed on the etched enamel treated with CS-AMEL hydrogel and MMP-20–CS-AMEL hydrogel (Fig. 2E to H). More important, highly organized and dense crystals parallel to each other along their *c*-axes were observed at higher magnification within the sample treated with MMP-20–CS-AMEL hydrogel (see arrows in Fig. 2H).

The mineral composition and orientation of the newly grown crystals were further confirmed by XRD (Fig. 3A). The XRD pattern of etched enamel was measured for comparison. All of the diffraction peaks at 2θ = 25.8 (002), 2θ = 31.6 (211), and 2θ = 32.6 (300) were indexed to hexagonal HAP (JCPDS 09-0432). The presence of sharp 002 diffraction peaks in both the CS-AMEL– and MMP-20–CS-AMEL–treated samples indicated that the apatite crystals were mutually parallel along the *c*-axis. The orientation degree of the synthetic apatite crystals was evaluated by analyzing the ratios of $I_{(002)}/I_{(211)}$, which were 0.5, 0.95, and 1.6 for samples treated with chitosan, CS-AMEL, and MMP-20–CS-AMEL hydrogel, respectively (Fig. 3B). As observed in SEM (Fig. 2), the increased $I_{(002)}/I_{(211)}$ ratios indicated an increased preferential orientation of apatite crystals when amelogenin and MMP-20 were added to the hydrogel. The crystallinity of newly formed crystals in the CS-AMEL hydrogel decreased to 19.6% from 37% in those grown without amelogenin. The decrease in crystallinity can be attributed to the presence of occluded proteins and ACP in the synthetic crystals, as has been demonstrated both in vitro and in vivo (Beniash et al. 2005, 2009; Kwak et al. 2011; Prajapati et al. 2016). In vitro studies have shown that full-length amelogenin stabilizes ACP and prevents its transformation into HAP (Kwak et al. 2011, 2016). As expected, the crystallinity increased to 35.6% when MMP-20 was added to the CS-AMEL hydrogel (Fig. 3C). Our in vivo examination of enamel crystals collected from *Mmp20*-null mice has revealed lower crystallinity and more imperfections as a result of protein occlusion compared with crystals from wild-type mice (Prajapati et al. 2016).

FTIR analysis was performed to identify additional components of the newly grown enamel. All spectra exhibited characteristic bands for HAP and chitosan (Fig. 3D; Brugnerotto et al. 2001; Tao 2013). In the spectrum of samples treated with CS-AMEL hydrogel, an Amide I shoulder was detected at ~1,630 $cm^{-1}$, indicating the presence of protein in the newly formed layers (arrow in Fig. 3D; Mallamace et al. 2015). The intensity of this Amide I shoulder was weak, and no other characteristic band for protein was observed in the FTIR spectrum. The faint protein signal in the IR spectrum can be attributed to the occlusion of protein within the newly formed crystals. A similar phenomenon has also been observed in the Raman and IR spectra of nanocomposites formed by incorporation of polymers in calcite crystals, which exhibited no characteristic band for polymers because of their occlusion within the calcite crystals (Kim, Semsarilar, et al. 2016). The Amide I shoulder disappeared in the spectrum of the newly grown enamel formed by MMP-20–CS-AMEL hydrogel. Moreover, the absorption bands corresponding to Amide II and III bands were observed at 1,590 and 1,453 $cm^{-1}$, respectively (Fig. 3E, F), revealing the presence of some proteolytic products of amelogenin in the newly formed layers (Mallamace et al. 2015).

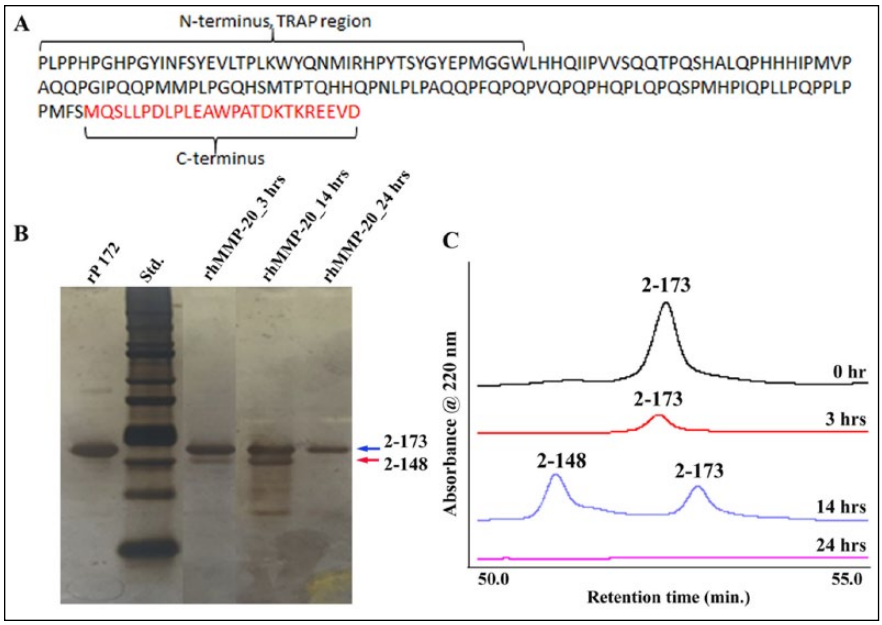


**Figure 1.** Proteolysis of amelogenin rP172 by MMP-20 in the chitosan hydrogel. (**A**) Primary amino acid sequence of recombinant porcine amelogenin showing the 20-kDa C-terminally cleaved P148 peptide (black font) and the cleaved C-terminus (red font). The first 44 amino acids from the N-terminal region constitute the tyrosine-rich amelogenin polypeptide (TRAP) region of amelogenin. (**B**) Sodium dodecyl sulfate polyacrylamide gel electrophoresis showing peptides obtained after proteolysis of amelogenin by rhMMP20 at 3, 14, and 24 h without chitosan hydrogel. Based on the full-length amelogenin rP172 (designated as I, amino acids 2 to 173, 25 kDa; Fig. 1A), the proteolytic products were designated as II, 2 to 148 (20 kDa), III, 46 to 148 (13 kDa; Moradian-Oldak et al. 2001; Sun et al. 2008). The major proteolytic product lacking the hydrophilic C-terminal 25 amino acids, namely, P148, appeared after 3 h of proteolysis, and its content was increased when the proteolysis time increased to 14 h. After 24 h, a full-length amelogenin band along with another band at 13 kDa persisted. The arrows represent the 20k peptide p148, and the full-length amelogenin (rp172). (**C**) Reverse-phase chromatography showing the amelogenin proteolysis products at various time intervals. This figure is available in color online.

## *Mechanical Properties of the Biomimetic Regrown Enamel*

Figures 3G and H show the elastic modulus and hardness of the HAP crystal layers in samples treated with chitosan, CS-AMEL, and MMP-20–CS-AMEL hydrogels. Acid etching of enamel resulted in a reduction in the hardness and modulus values. After mineralization with chitosan hydrogel, there was no significant difference in the mechanical properties of the newly formed layer. A 2.6-fold increase in the elastic modulus and a 2.4-fold increase in hardness were observed in the HAP crystals grown in CS-AMEL hydrogel. When MMP-20 was added, there was an increase in the modulus of elasticity and hardness of the newly grown layers, and a 1.8-fold increase in elasticity (Fig. 3G) and a 2.4-fold increase in the hardness (Fig. 3H) were observed compared with the etched enamel repaired by CS-AMEL hydrogel without MMP-20.

## Discussion

Enamel formation involves a series of highly regulated molecular events and protein-controlled mineralization processes concomitant with enzymatic activities. Here, the introduction of MMP-20 to the CS-AMEL hydrogel for enamel regrowth was aimed to simulate natural conditions. During enamel formation, the newly secreted amelogenin is cleaved by MMP-20 at its C-terminal, promoting the process of HAP crystal formation and facilitating enamel hardening (Bartlett and Simmer 1999). We confirmed that the full-length rP172 amelogenin was cleaved by MMP-20 at the C-terminus to produce a P148 polypeptide in the MMP-20–CS-AMEL system.

Studies on *Mmp20*-null mice have documented the importance of proteolytic processing and its role in normal enamel development (Caterina et al. 2002). A mutation in the MMP-20 active site results in hypomaturation *Amelogenesis Imperfecta* (Ozdemir et al. 2005; Kim et al. 2017), a dental phenotype in which the enamel is softer than normal and contains residual enamel proteins. Enamel in *Mmp20*-null mice is hypoplastic and hypomineralized and has an altered enamel rod pattern. Analysis of teeth from *Mmp20*-null mice showed that 1) the *Mmp20*-null mouse had an overall 50% decrease in mineral content as compared with the wild type (Smith et al. 2011), 2) the amount of proteins and water content in *Mmp20*-null mouse increased to almost twice that of the wild type, and 3) kallikrein-4 was not able to compensate for the loss of MMP-20 (Bartlett et al. 2004). In our recent analysis of apatite crystals isolated from *Mmp20*-null mice, we confirmed that the absence of MMP-20

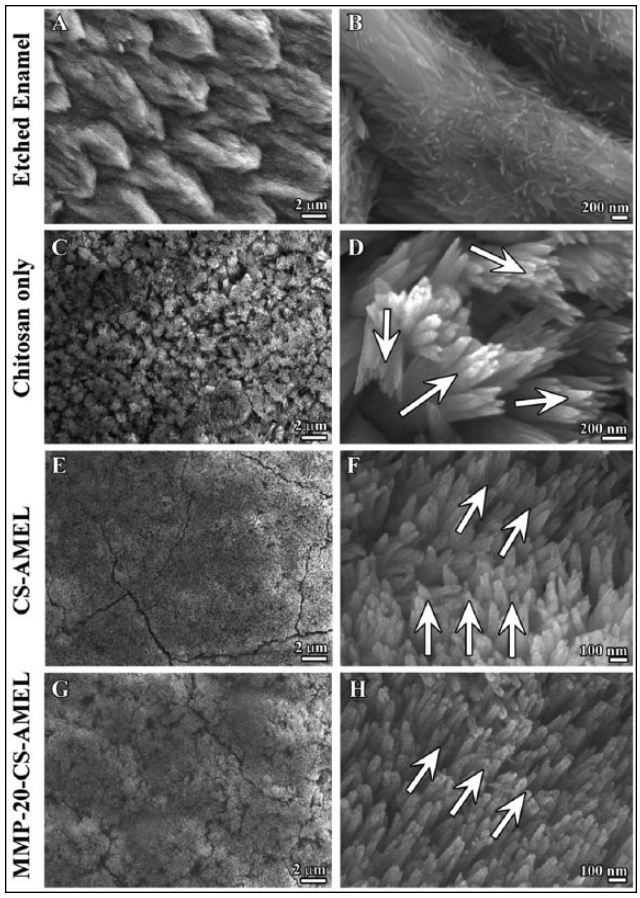


**Figure 2.** Microstructure of enamel-like apatite crystals in the newly grown layer. Scanning electron micrography images showing (**A, B**) etched enamel, newly grown hydroxyapatite crystals in chitosan hydrogel (**C, D**), amelogenin-chitosan hydrogel (**E, F**), and amelogenin-chitosan hydrogel with matrix metalloproteinase–20 (**G, H**). Arrows in D, H, and F indicate the crystal orientation.

during amelogenesis resulted in the occlusion of proteins inside the HAP crystals, which affected their morphology, crystallinity, and consequently enamel mechanical properties (Prajapati et al. 2016).

The development of CS-AMEL hydrogel for biomimetic enamel repair was inspired by the important role of amelogenin in controlling oriented and elongated growth of enamel crystals. We have previously reported that the thickness of the newly grown layer was about 15 to 30 μm after 5 or 7 d of treatment (Ruan et al. 2013; Mukherjee et al. 2016). To improve the clinical applicability of the hydrogel, research in our laboratory is in progress to increase the thickness of the regrown layers.

Consistent with our previous results (Ruan et al. 2013, 2014), here the CS-AMEL hydrogel promoted the formation of organized needle-like HAP crystals with increased orientation compared with crystals formed without amelogenin. This oriented crystal arrangement has been suggested as one of the major contributions to the exceptional mechanical properties of enamel (Braly et al. 2007; An et al. 2012). We have observed a significant improvement in both elastic modulus and hardness of repaired enamel treated with CS-AMEL hydrogel compared with samples remineralized without amelogenin. However, during biomimetic enamel remineralization, unlike the natural process of enamel formation, the amelogenin may become trapped inside the growing apatite crystals because of a lack of proteinases (Prajapati et al. 2016). As a result, the occlusion of proteins may have unfavorable effects on the organization and crystallinity of newly formed crystals and limit the mechanical performance of the artificial enamel.

The stepwise processing of amelogenin by MMP-20 in the CS-AMEL hydrogel during the biomimetic enamel regrowth enhances crystal formation in multiple ways. Proteolytic activities of MMP-20 may affect amelogenin-apatite interactions by producing intermediate products that have less affinity for apatite and affect crystal morphology in different ways (Iijima and Moradian-Oldak 2004; Sun et al. 2008). An in vitro study proposed that MMP-20–induced proteolysis of full-length native amelogenin could help regulate the transformation of ACP into ordered arrays of apatite crystals (Kwak et al. 2011, 2016). This action of MMP-20 guides the growth morphology of forming HAP crystals and enhances their crystallinity. We therefore propose that the proteolysis of amelogenin by MMP-20 added to CS-AMEL hydrogel regulates crystal formation by 1) triggering the ACP-to-apatite phase transformation guided by amelogenin (Kwak et al. 2016), 2) preventing unwanted protein occlusion inside apatite crystals (Prajapati et al. 2016), and 3) decreasing the amelogenin-apatite binding affinity to allow growth (Sun et al. 2008). MMP-20 in the CS-AMEL hydrogel also increased the organization of the newly formed crystals. It has been proposed that full-length amelogenin and its cleavage products undergo a dynamic coassembly process that allows the programmed growth of elongated apatite crystals in a hierarchically organized manner (Yang et al. 2011). This assertion raises the possibility that HAP crystals may affect the activity of MMP-20 on enamel matrix proteins during amelogenesis (Sun et al. 2010). More Ca and $PO_4$ ions precipitated in the mineralization system throughout the course of the experiment in the presence of MMP-20 (Uskoković et al. 2011). Similar events may be occurring in our in vitro regrowth experiments, resulting in more organized crystal growth in the presence of MMP-20. The precise organic-inorganic composition of biocomposites as well as their crystallinity and organization are well known to be important factors that influence their mechanical properties (Zhang et al. 2014; Kim, Carloni, et al. 2016). In our study, a marked increase in the hardness and modulus of elasticity of the newly grown crystals was observed after the addition of MMP-20 to the CS-AMEL remineralization system.

In summary, we demonstrate that addition of MMP-20 to CS-AMEL hydrogel improved the composition, structure, and mechanical properties of the artificial enamel. As a result of proteolysis of amelogenin by MMP-20 during the biomimetic enamel regrowth, the newly grown enamel-like layer exhibited well-regulated crystal growth, and protein occlusion was prevented. Although future work is needed to further incorporate other enamel matrix proteins into the system, this study brings us a step closer to growing artificial enamel.

## Author Contributions

S. Prajapati, contributed to conception, design, data acquisition, analysis, and interpretation and drafted and critically revised the manuscript; Q. Ruan, contributed to conception, design, data

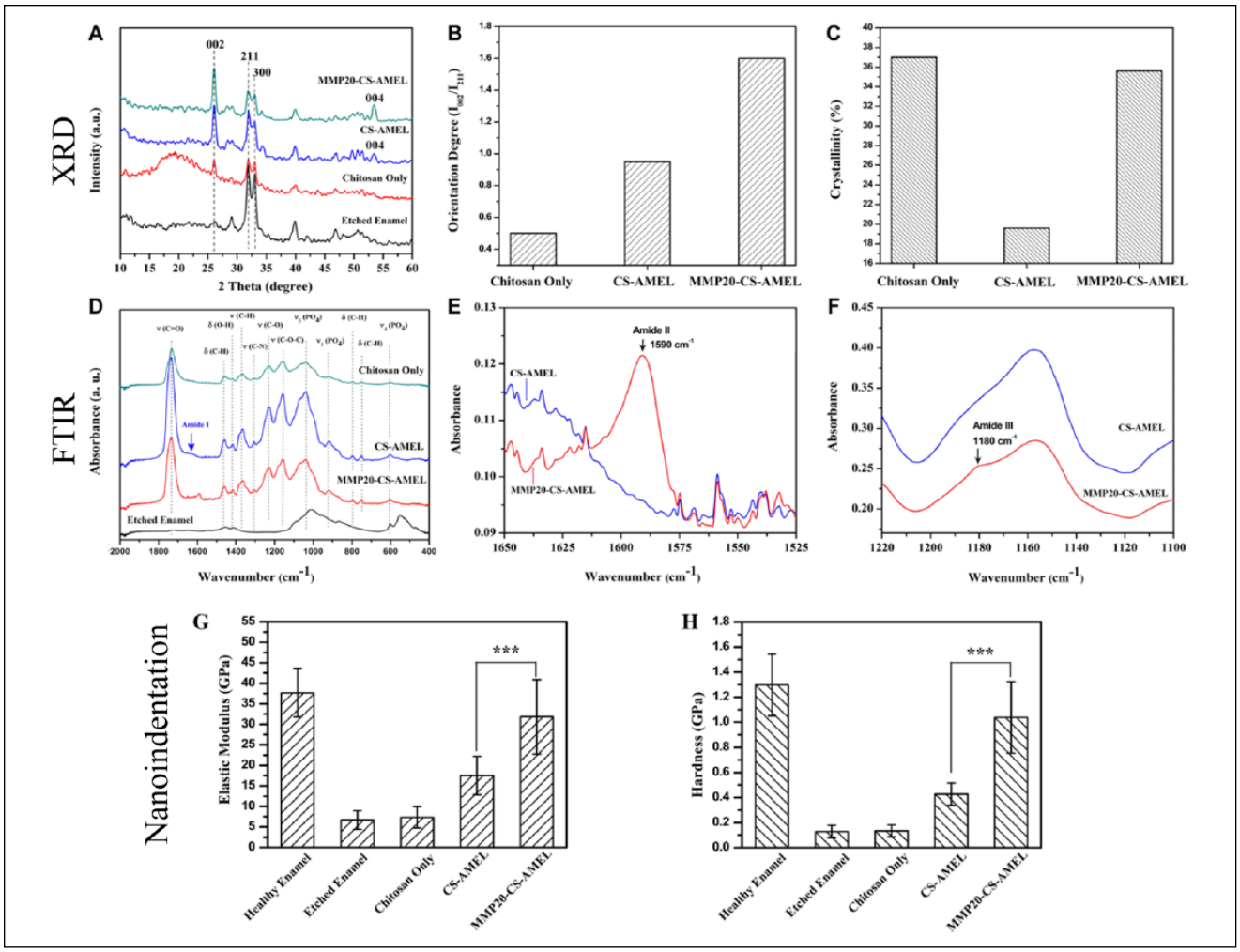


**Figure 3.** Composition, orientation, and mechanical properties of the newly grown layer. (**A**) X-ray diffraction patterns of etched enamel and newly grown layer grown in chitosan, amelogenin-chitosan, and matrix metalloproteinase–20 (MMP-20) containing amelogenin-chitosan hydrogel. Diffraction peaks at $2\theta = 25.8$ (002), $2\theta = 31.6$ (211), and $2\theta = 32.6$ (300) can be readily indexed to hexagonal phase hydroxyapatite (JCPDS 09-0432). (**B**) Orientation degrees and (**C**) crystallinity of newly grown crystals formed in chitosan, amelogenin-chitosan, and amelogenin-chitosan hydrogel containing MMP-20. (**D**) Fourier transform infrared (FTIR) spectra of etched enamel, newly grown layer formed in chitosan, amelogenin-chitosan, and amelogenin-chitosan hydrogel with MMP-20. The characteristic bands for hydroxyapatite appeared at 1,000 to 1,120 $cm^{-1}$ ($\nu_3$ [$PO_4$]), 916 $cm^{-1}$ ($\nu_1$ [$PO_4$]), and 601 $cm^{-1}$ ($\nu_4$ [$PO_4$]; Tao 2013). The characteristic peaks for chitosan were found at 1,735 $cm^{-1}$ ($\nu$ [C=O]), 1,458 $cm^{-1}$ ($\delta$ [C-H]), 1,418 $cm^{-1}$ ($\delta$[O-H]), 1,365 $cm^{-1}$ ($\nu$ [C-H]), 1306 $cm^{-1}$ ($\nu$ [C-N]), 1,228 $cm^{-1}$ ($\nu$ [C-O]), 1,156 $cm^{-1}$ ($\nu$ [C-O-C]), 798 ($\delta$[C-H]), 752 $cm^{-1}$ ($\delta$[C-H]; Brugnerotto et al. 2001). (**E, F**) FTIR spectra of newly grown layer formed in amelogenin-chitosan hydrogel (blue) and MMP-20–amelogenin-chitosan hydrogel (red) representing the (B) Amide II and (V) Amide III regions. (**G, H**) Elastic modulus and hardness of healthy enamel, etched enamel, and repaired enamel treated with chitosan, amelogenin-chitosan, and amelogenin-chitosan hydrogel containing MMP-20. ***$P < 0.001$. This figure is available in color online.

acquisition, and analysis and drafted and critically revised the manuscript; K. Mukherjee and S. Nutt, contributed to data acquisition and analysis and critically revised the manuscript; J. Moradian-Oldak, contributed to design, data analysis, and interpretation and critically revised the manuscript. All authors gave final approval and agree to be accountable for all aspects of the work.

## Acknowledgments

This research was supported by the National Institutes of Health/National Institute of Dental and Craniofacial Research grants R01-DE-13414 and R01-DE-020099, the University of Southern California (USC) Coulter Translational Partnership Program, and the 2015 GSK-IADR innovation in Oral Care Award to J.M.-O. The authors would like to thank the Center for Electron Microscopy and Microanalysis at USC for electron microscopy. The authors declare no potential conflicts of interest with respect to the authorship and/or publication of this article.

## References

An BB, Wang RR, Zhang DS. 2012. Role of crystal arrangement on the mechanical performance of enamel. Acta Biomater. 8(10):3784–3793.

Bartlett J, Simmer J. 1999. Proteinases in developing dental enamel. Crit Rev Oral Biol Med. 10(4):425–441.

Bartlett JD, Beniash E, Lee DH, Smith CE. 2004. Decreased mineral content in MMP-20 null mouse enamel is prominent during the maturation stage. J Dent Res. 83(12):909–913.

Beniash E, Metzler RA, Lam RSK, Gilbert P. 2009. Transient amorphous calcium phosphate in forming enamel. J Struct Biol. 166(2):133–143.
Beniash E, Simmer JP, Margolis HC. 2005. The effect of recombinant mouse amelogenins on the formation and organization of hydroxyapatite crystals in vitro. J Struct Biol. 149(2):182–190.
Braly A, Darnell LA, Mann AB, Teaford MF, Weihs TP. 2007. The effect of prism orientation on the indentation testing of human molar enamel. Arch Oral Biol. 52(9):856–860.
Brugnerotto J, Lizardi J, Goycoolea FM, Argüelles-Monal W, Desbrières J, Rinaudo M. 2001. An infrared investigation in relation with chitin and chitosan characterization. Polymer. 42(8):3569–3580.
Caterina JJ, Skobe Z, Shi J, Ding Y, Simmer JP, Birkedal-Hansen H, Bartlett JD. 2002. Enamelysin (Mmp-20) deficient mice display an *amelogenesis imperfecta* phenotype. J Biol Chem. 277:49598–49604.
Iijima M, Moradian-Oldak J. 2004. Control of octacalcium phosphate and apatite crystal growth by amelogenin matrices. J Mater Chem. 14(14):2189–2199.
Kim YJ, Kang J, Seymen F, Koruyucu M, Gencay K, Shin TJ, Hyun HK, Lee ZH, Hu JC, Simmer JP, et al. 2017. Analyses of MMP20 missense mutations in two families with hypomaturation amelogenesis imperfecta. Front Physiol. 8:229.
Kim YY, Carloni JD, Demarchi B, Sparks D, Reid DG, Kunitake ME, Tang CC, Duer MJ, Freeman CL, Pokroy B, et al. 2016. Tuning hardness in calcite by incorporation of amino acids. Nat Mater. 15(8):903–910.
Kim Y-Y, Semsarilar M, Carloni JD, Cho KR, Kulak AN, Polishchuk I, Hendley CT, Smeets PJM, Fielding LA, Pokroy B, et al. 2016. Structure and properties of nanocomposites formed by the occlusion of block copolymer worms and vesicles within calcite crystals. Adv Func Mater. 26(9):1382–1392.
Kwak SY, Green S, Wiedemann-Bidlack FB, Beniash E, Yamakoshi Y, Simmer JP, Margolis HC. 2011. Regulation of calcium phosphate formation by amelogenins under physiological conditions. Eur J Oral Sci. 119(Suppl. 1):103–111.
Kwak SY, Yamakoshi Y, Simmer JP, Margolis HC. 2016. MMP20 proteolysis of native amelogenin regulates mineralization in vitro. J Dent Res. 95(13):1511–1517.
Landi E, Tampieri A, Celotti G, Sprio S. 2000. Densification behaviour and mechanisms of synthetic hydroxyapatites. J Eur Ceram Soc. 20(14–15):2377–2387.
Mallamace F, Corsaro C, Mallamace D, Vasi S, Vasi C, Dugo G. 2015. The role of water in protein's behavior: the two dynamical crossovers studied by NMR and FTIR techniques. Comput Struct Biotechnol J. 13:33–37.
Mann S. 1997. The biomimetics of enamel: a paradigm for organized biomaterials synthesis. Chichester (UK): John Wiley & Sons.
Moradian-Oldak J. 2009. The regeneration of tooth enamel. Dimens Dent Hyg. 7(8):12–15.
Moradian-Oldak J. 2012. Protein-mediated enamel mineralization. Front Biosci (Landmark Ed). 17:1996–2023.
Moradian-Oldak J, Jimenez I, Maltby D, Fincham AG. 2001. Controlled proteolysis of amelogenins reveals exposure of both carboxy- and amino-terminal regions. Biopolymers. 58(7):606–616.
Mukherjee K, Ruan Q, Liberman D, White SN, Moradian-Oldak J. 2016. Repairing human tooth enamel with leucine-rich amelogenin peptide-chitosan hydrogel. J Mater Res. 31(5):556–563.
Nanci A, ed. 2013. Enamel: composition, formation, and structure. In: Ten cate's oral histology development, structure, and function. 8th ed. St. Louis (MO): Elsevier Mosby. p. 122.
Ozdemir D, Hart PS, Ryu OH, Choi SJ, Ozdemir-Karatas M, Firatli E, Piesco N, Hart TC. 2005. MMP20 active-site mutation in hypomaturation amelogenesis imperfecta. J Dent Res. 84(11):1031–1035.
Palmer LC, Newcomb CJ, Kaltz SR, Spoerke ED, Stupp SI. 2008. Biomimetic systems for hydroxyapatite mineralization inspired by bone and enamel. Chem Rev. 108(11):4754–4783.
Prajapati S, Tao J, Ruan Q, DeYoreo JJ, Moradian-Oldak J. 2016. Matrix metalloproteinase-20 mediates dental enamel biomineralization by preventing protein occlusion inside apatite. Biomaterials. 75:260–270.
Ruan Q, Moradian-Oldak J. 2014. Development of amelogenin-chitosan hydrogel for in vitro enamel regrowth with a dense interface. J Vis Exp. 2014;89.
Ruan Q, Moradian-Oldak J. 2015. Amelogenin and enamel biomimetics. J Mater Chem B Mater Biol Med. 3:3112–3129.
Ruan Q, Siddiqah N, Li X, Nutt S, Moradian-Oldak J. 2014. Amelogenin-chitosan matrix for human enamel regrowth: effects of viscosity and supersaturation degree. Conn Tissue Res. 55(suppl. 1):150–154.
Ruan Q, Zhang Y, Yang X, Nutt S, Moradian-Oldak J. 2013. An amelogenin-chitosan matrix promotes assembly of an enamel-like layer with a dense interface. Acta Biomater. 9(7):7289–7297.
Smith CE, Hu Y, Richardson AS, Bartlett JD, Hu JC, Simmer JP. 2011. Relationships between protein and mineral during enamel development in normal and genetically altered mice. Eur J Oral Sci. 119(suppl. 1):125–135.
Sun Z, Ahsan MM, Wang H, Du C, Abbott C, Moradian-Oldak J. 2006. Assembly and processing of an engineered amelogenin proteolytic product (rP148). Eur J Oral Sci. 114(suppl. 1):59–63.
Sun Z, Carpiaux W, Fan D, Fan Y, Lakshminarayanan R, Moradian-Oldak J. 2010. Apatite reduces amelogenin proteolysis by MMP-20 and KLK4 in vitro. J Dent Res. 89(4):344–348.
Sun Z, Fan D, Fan Y, Du C, Moradian-Oldak J. 2008. Enamel proteases reduce amelogenin-apatite binding. J Dent Res. 87(12):1133–1137.
Tao J. 2013. FTIR and Raman studies of structure and bonding in mineral and organic-mineral composites. Methods Enzymol. 532:533–556.
Uskoković V, Khan F, Liu H, Witkowska HE, Zhu L, Li W, Habeliz S. 2011. Hydrolysis of amelogenin by matrix metalloprotease-20 accelerates mineralization in vitro. Arch Oral Biol. 56(12):1548–1559.
Yang X, Sun Z, Ma R, Fan D, Moradian-Oldak J. 2011. Amelogenin "nanorods" formation during proteolysis by Mmp-20. J Struct Biol. 176(2):220–228.
Yang X, Wang L, Qin Y, Sun Z, Henneman ZJ, Moradian-Oldak J, Nancollas GH. 2010. How amelogenin orchestrates the organization of hierarchical elongated microstructures of apatite. J Phys Chem B. 114(6):2293–2300.
Zhang YR, Du W, Zhou XD, Yu HY. 2014. Review of research on the mechanical properties of the human tooth. Int J Oral Sci. 6(2):61–69.